Properties of small clusters at ionic surfaces: $(NaCl)_n$ clusters ($n = 1-48$) at the (100) MgO surface

Alexander L. Shluger
The Royal Institution of Great Britain, 21 Albemarle Street, London W1X 4BS, United Kingdom and Institute of Chemical Physics, University of Latvia, 19 Rainis Boulevard, Riga 1098, Latvia

Andrew L. Rohl and David H. Gay
The Royal Institution of Great Britain, 21 Albemarle Street, London W1X 4BS, United Kingdom
(Received 17 October 1994; revised manuscript received 13 January 1995)

We have studied the geometry, binding energy, interaction with the surface, barriers for diffusion, optical absorption, and the possibility for their observation using atomic force microscopy of $(NaCl)_n$ clusters ($n = 1-48$) on the (100) MgO surface. We address the questions at which cluster size do the adsorbed molecules lose their identity and how do strained clusters accommodate the strain. The relation between the structure of initial molecular fragments adsorbed at the surface and the structure of the corresponding thick film is discussed. The results are compared with the calculated structures of the free clusters and the experimental data on the molecular-beam epitaxy of alkali halides.

I. INTRODUCTION

Elemental and molecular clusters are often considered to bridge the gap between the properties and behavior of single molecules in the gas phase and bulk condensed matter.[1-4] In particular, small molecular clusters of ionic compounds are the focus of many experimental and theoretical studies. Interest in these systems is prompted first of all by their relatively simple structure. Free clusters of various sizes can be readily produced in laser-vaporization sources,[5] by gas aggregation,[6] and particle sputtering.[7] The formation, size, structure, and chemical properties of charged clusters of alkali halides[5,8-12] (AH's) and cubic oxides such as MgO and CaO (Refs. 6,13-16) have been investigated experimentally in great detail. Atomic and electronic structures of free small alkali halide and oxide clusters have been calculated using different techniques.[17-25]

Despite the increasing number of studies of the properties of free molecular clusters, the experimental techniques applicable for the study of their geometric and electronic structures are limited. In particular, the analysis of the mass spectra of charged nonstoichiometric clusters[5] provides only qualitative information regarding the geometric models of these clusters. Recent advances in the molecular-beam epitaxy (MBE) growth of insulators and the possibility of cluster deposition at insulating surfaces offer new opportunities in this respect: clusters can be deposited directly on surfaces from the cluster source[10] or formed during homo- and heteroepitaxial growth of ionic compounds.[26-30] Their structure can be studied using a wide range of techniques including such methods as atomic force microscopy[31-33] (AFM) and ion and metastable-atom impact electron spectroscopy[34] (IIES and MIES). Apart from the clear fundamental interest, information obtained in these studies could provide an insight into the mechanisms of crystal film growth, homo- and heteroepitaxy, structural and electronic characteristics of nanoscopic species and their interaction with surfaces, and properties of surface inhomogeneities, including steps and kinks. This information could be used in order to estimate the accuracy and resolution of the surface-sensitive techniques such as AFM, IIES, and MIES.

Theoretically, Bjorklund and co-workers considered reactions between alkali halide molecular beams (mainly AH molecules and dimers) and single crystals of alkali halides.[35-37] Shluger, Gale, and Catlow studied absorption of MgO and LiCl molecules at the (100) MgO surface.[38] Celli and Urzua calculated the configurations of adsorbed NaCl and KBr molecules on the (100) NaCl and (100) KBr surfaces.[39] No theoretical studies have examined larger clusters on surfaces to our knowledge.

In this study we consider some general features concerning the structure and diffusion of molecular clusters at ionic surfaces with large geometric misfit using atomistic simulation and quantum-chemical techniques. A good geometric and chemical contrast between the host surface and point defects, such as impurities and adsorbed molecules and clusters, is necessary for their observation using AFM and spectroscopic techniques. As a particular system we have chosen NaCl clusters on the (100) MgO surface. MgO is known as a good support for deposition of different molecules and heteroepitaxial growth of other materials. It provides an example of a cubic ionic material with a strong crystalline field near the surface. The latter should make the adsorption energies large and emphasize the strain effects in which we are interested in this study. Formal misfit between the lattice constants of MgO and NaCl is about 6:8. We analyze the calculated properties of $(NaCl)_n$ clusters ($n = 1-48$) at the MgO surface from the point of view of their geometry, binding energy, barriers for diffusion, optical absorption, and the possibility of their observation using AFM. Dynamic processes of the interaction of molecules and clusters with surfaces are beyond the scope of this paper. Although at real surfaces the molecules often fill the defective sites such as kinks, vacancies, and step edges first, in this study we will focus on their interaction with perfect surfaces.

II. CALCULATION TECHNIQUES

We report the results of static calculations based on total-energy minimization to obtain the equilibrium cluster geometries and adiabatic barrier energies for cluster diffusion, which do not take into account energy dissipation in the adsorption and cluster formation process. The large number of relaxing ions requires a semiempirical technique for energy calculation. Therefore we have employed both an atomistic simulation technique (MARVIN code[40,41]), and a semiempirical quantum-chemical method (CLUSTER code[42–44]).

A. MARVIN atomistic simulation technique

This technique adopts a multiblock approach, with planar two-dimensional periodic boundary conditions parallel to the interface. Each block consists of two regions as shown in Fig. 1. The first contains the ions which are relaxed explicitly until there is zero force on each of them, while the ions in the second are fixed. Thus the model of a surface consists of a block (A) with its region 1 containing the ions closest to the surface, and the ions in region 2 are fixed to reproduce the potential of the remaining lattice (see Fig. 1). The methodology is closely related to that used by Tasker[45] in the MIDAS code. In the adsorption calculations, the adsorbing molecules are placed in the same block as the surface ions and all ions of the adsorbed cluster and the surface layer are allowed to relax. In all the MARVIN calculations of adsorption in this study, the surface region 1 contained one plane of 200 surface ions and the cluster ions. Region 2 contained four planes of frozen ions. The surface deformation due to the cluster-surface interaction in the present work did not exceed $0.08a$ (a is the lattice interionic distance) perpendicular to the surface plane. Based on our previous AFM calculations[41] using the same technique, in which the surface deformation was much larger, we believe that additional unfrozen surface planes would not change our qualitative conclusions.

To speed up the calculations, we have incorporated the idea of "freezing." This involves taking an ion out of the minimization if the force on it is less than a given value. There is no guarantee that the force on this ion will not increase as the rest of the ions relax around it, and this is checked for at the end of each calculation. This technique has been found to be extremely effective for the calculations presented here.

The functional forms of the potentials used to describe the clusters and surface and their interaction are based on an ionic model. The major interaction is between charges centered on the positions of the ions, with electronic polarizability incorporated via the Dick-Overhauser shell model.[46] The Coulomb interaction is long range and the sum over the crystal lattice is conditionally convergent. Hence a two-dimensional Ewald summation technique has been employed.[47,48] Two-body potentials were used to represent the non-Coulombic interactions between the ions. The range over which these non-Coulombic interactions operate is determined by a potential cutoff.

The parameters of the pair potentials used in this work ar summarized in Table I. The short-range potentials for most of the ions were specially optimized. The aim of this optimization was to maintain the consistency between the different interactions and to reproduce the characteristics of the perfect lattices correctly but still produce a potential whose functional form is robust with respect to significant distortions in the bond lengths away from equilibrium values. In particular, the oxygen-oxygen potential was determined by simultaneously fitting the short-range parameters to reproduce the lattice parameters of a range of different binary and ternary oxides.[49] All other potentials were initially derived using an electron-gas method and further refined by fitting to the perfect-lattice properties of the appropriate materials, e.g., MgO, NaCl, Na_2O, $MgCl_2$. Since these are fitted to experimental data, they can be described as "empirical" potentials. In cases where no lattice data were available (i.e., for O-Cl, Mg-Na), an empiricizing procedure was employed[50] described as follows using O-Cl as an example. The short-range energies between O-Cl and between

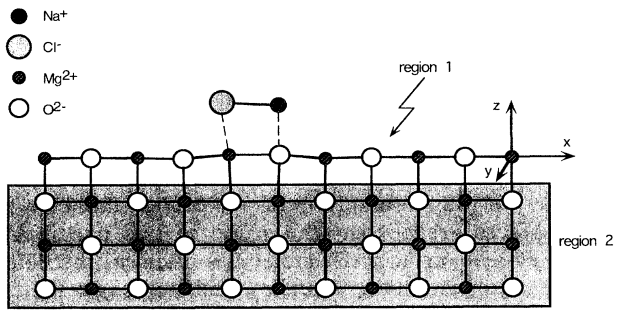

FIG. 1. Part of the simulation cell for the calculation of the adsorption of a molecule of NaCl onto the (100) plane of MgO. The cell is repeated infinitely in the x and y directions.

TABLE I. Short-range potentials used. The potentials have the functional forms $W(r)=A\exp(-r/\rho)$ (Born-Mayer) and $W(r)=A\exp(-r/\rho)+C/r^6$ (Buckingham).

Between ions	Potential type	A (eV)	ρ Å	C (eV Å^{-6})
O-O	Buckingham	9 574.96	0.2192	32.0
Na-O	Born-Mayer	1 677.83	0.2934	
Mg-O	Born-Mayer	1 284.38	0.2997	
Cl-O	Buckingham	4 393.1	0.2721	62.2
Cl-Cl[a]	Buckingham	2 021.3	0.3588	88.98
Na-Cl	Buckingham	3 046.4	0.2836	12.82
Mg-Cl	Buckingham	2 511.51	0.2857	6.22
Na-Na	Buckingham	6 927.8	0.1836	4.43
Na-Mg	Buckingham	28 261.4	0.1510	2.10

[a]The geometries of the small clusters are better reproduced without the short-range Cl-Cl interaction as it is fitted for the infinite lattice. Therefore this potential was only used to derive the Cl-O short-range potential. It was not used in the calculations of the cluster geometries, where only Coulomb repulsion was included.

Cl-Cl were calculated using an electron-gas method.[51] Although the absolute energies of these potentials are not consistent with the empirically derived potentials, the difference between electron-gas-derived potentials is assumed to be useful. As such, if the difference between the O-Cl and Cl-Cl electron-gas potentials is added to the empirical Cl-Cl potential, the resulting "empiricized" O-Cl potential is representative and consistent with the empirical potentials. For all anion-anion potentials, the C_6 dispersion terms were determined using the Kirkwood-Slater formulas.[52] Only Coulomb repulsion was taken into account for the Mg-Mg interaction. All the ions had their full formal charges and only the anions O and Cl were treated as polarizable. Their shell-model parameters[46,53] were the following: $Y_O = -2.04e$; $K_O = 6.3$; $Y_{Cl} = -1.984e$; $K_{Cl} = 13.209$ eV Å^{-2}.

Using the MARVIN code and this set of parameters we calculated the reconstructions of the perfect (001) surfaces of NaCl and MgO. The results are qualitatively similar for both crystals: the cations displace slightly inward and the anions outward from the crystal perpendicular to the ideal surface plane. The magnitudes of these displacements are about $0.01a$ (a is the bulk interionic separation) for MgO, and about $0.02a$ for NaCl. A very similar surface relaxation was calculated for MgO using the MIDAS code[54] and the CLUSTER code.[44]

To calculate the cluster-surface interaction energy and the cluster distortion at the surface we have also calculated the energetic and geometric parameters of the free clusters using interatomic potentials and the GULP code.[55] For comparison with the studies of free clusters we used the results of extensive Hartree-Fock *ab initio* calculations reported in Ref. 22 as they contain all the necessary numerical information. The latter is also necessary to check the parameters of our interatomic potentials. Agreement of the geometric parameters obtained is better than 5%. However, the binding energies calculated using interatomic potentials are generally about 10% bigger than those obtained using the Hartree-Fock method in Ref. 22. More detailed comparison of these results is presented in the next section.

B. CLUSTER quantum-chemical technique

The program employs both the embedded molecular cluster (EMC) model[38] and the periodic large unit cell (LUC) method[43,56] and is based on the intermediate neglect of differential overlap (INDO) approximation of the unrestricted Hartree-Fock-Roothaan method.[44,57] It allows us to determine the electronic structure of a quantum-mechanically described cluster that contains several tens of ions. It employs a minimal valence Slater basis set and uses a single-determinantal approximation for the wave function and therefore does not take into account van der Waals interactions. The lattice relaxation in the present study includes only ionic displacements from the lattice sites. The optical-absorption energies were calculated using the configuration-interaction technique and included all single-electron excitations.[58]

The calculation scheme of the CLUSTER code and the parametrization of the INDO method are described in Ref. 44. The procedure for a defect study on a crystal surface using the CLUSTER code includes the following steps. (1) Calculation of the electronic structure and relaxation of the perfect surface are made using periodic boundary conditions where the crystal surface is treated as a slab comprising several atomic planes. For this purpose the LUC method is used, as both sides of the two-dimensional infinite slab are equivalent. As has been shown both in our previous semiempirical calculations,[59] and in recent *ab initio* studies,[60] a slab comprising 5–7 atomic planes of the rocksalt ionic crystal lattice satisfies these requirements. (2) A study of adsorbtion on the surface is performed in the EMC model for a cluster embedded in a slab and adsorbed molecules. The atomic structure of the slab outside the cluster is treated as in the first step of the study. The ions outside the cluster carry the same basis of atomic orbitals (AO's) as inside the cluster, but with the Löwdin populations[57] of those AO's frozen to the AO populations in the slab simulating the perfect surface. The Coulomb interaction with these ions is calculated exactly up to a distance R where the Coulomb integral between two interacting points becomes practically equal to $1/R$. The potential of the crystalline field produced by the rest of the slab is then calculated using the Ewald method.[47] The crystal surface in the EMC calculations was simulated by a $Na_{48}Cl_{48}$ molecular cluster comprising one plane of 96 ions embedded in the slab of five lattice planes.

Finally we should make some comments regarding the accuracy of the results of the present calculations. First, the interaction energy between the periodically located clusters can be considerable. However, it was not bigger than 0.03 eV in our calculations even for the largest 48-molecule cluster. Secondly, the energy of the van der Waals interaction between the cluster and their surface depends on the number of surface layers as it decreases very slowly. However, as is shown below, the geometry of the clusters at the surface does not depend significantly on the van der Waals interaction. Therefore a five-layer slab was used in all MARVIN calculations. Thirdly, the charges on the ions are fixed in all MARVIN calculations. However, they may be different for the cluster ions with different coordination,[38] and for the surface ions interacting with the cluster. As was obtained in the quantum-chemical calculations of the clusters at the surface using the CLUSTER code, the variation in the charge values does not exceed $0.05e$ (e is the electron charge). Therefore we believe that this cannot change our qualitative conclusions.

III. RESULTS OF CALCULATIONS

The cluster structure to a certain extent is determined by the surface, and the variety of possible cluster structures formed at surfaces, although large for large number of molecules, can be much smaller than that for free clusters. In this study we did not consider all possible cluster structures for a given number of molecules, but rather addressed some specific issues regarding clusters at surfaces.

A. Which structural fragments can one expect at the very initial stages of molecule aggregation?

Adsorption of individual AH and MgO molecules at the (100) surfaces of AH and MgO has been considered in a number of studies using different calculation techniques.[36,38,39] At long surface-molecule distances their interaction is determined by the exponentially decaying electrostatic field of the whole surface. At short (about the crystal lattice constant) distances the ions of the molecule interact with the individual surface ions by the strong Coulomb and short-range forces. Finally, the molecule adopts a distorted configuration with the positively charged ion roughly above the surface anion and the negatively charged anion above the surface cation (see Fig. 1). This configuration reflects the predominance of the electrostatic forces.

The properties of the whole system "the surface with adsorbed molecular cluster" are determined by its free energy.[61] In this study we approximately determined the relative stability of the different configurations of the clusters comprising the same number of molecules at the surface by comparing the total energies of the system. Another useful energetic parameter which characterizes the cluster-surface interaction is the molecule (cluster) adsorption energy E_{ad} at the surface. It is defined with respect to the free state of the cluster with the same shape (if it exists) as stabilized at the surface. This energy includes the surface, E_{sur}^{rel}, and molecule (cluster), E_{cl}^{rel}, distortion energies with respect to their free states, and the molecule-surface interaction energy E_{int} at the equilibrium configuration of the adsorption:

$$E_{ad}=E_n-E_{sur}^0-E_{cl}^0=E_{int}+(E_{sur}^{rel}+E_{cl}^{rel}) ,$$

where E_n is the total energy of the surface with n adsorbed molecules, and E_{sur}^0 and E_{cl}^0 are the energies of the relaxed free surface and cluster, respectively. The adsorption energy of the single NaCl molecule at the (100) MgO surface obtained in our calculations is equal to 1.01 eV. As can be seen in Table II, the surface distortion energy due to adsorption of the NaCl molecule is about ten times bigger than the molecule distortion energy. The nearest surface ions are considerably displaced from their positions at the perfect surface (see Fig. 1) due to the strong dipole-surface and short-range interactions with the molecule, whereas the intramolecular distance increases from 2.47 to 2.53 Å. The biggest displacements of the surface ions are those perpendicular to the surface plane and comprise $0.07a$ and $0.08a$ for the O and Mg ion, respectively, where a is the Mgo bulk interionic separation ($a=2.1058$ Å in our calculations).

Displaced surface ions and adjacent vacancies considerably change the surface electrostatic potential which decreases much more slowly than that of the perfect surface. The interaction of the molecule dipole moment with this potential determines the large molecule-surface interaction energy. For instance, the latter is equal to only -0.35 eV for the molecule interacting with the rigid perfect surface. It is interesting to note that the gain in the molecule-surface interaction energy due to the surface distortion considerably outweighs the surface distortion energy. This explains why the surface of hard MgO distorts so readily in the field of a molecule.

The mobility of the molecules at the surface is one of

TABLE II. Adsorption, cluster, surface relaxation, and cluster-surface interaction energies in eV for selected clusters. E_{cl}^{rel}/N is the cluster relaxation per molecule. Missing energies do not have corresponding free clusters with the same shape as at the surface. Entries marked with an asterisk correspond to the most stable cluster configurations at the surface calculated in this study for a given number of molecules.

N	Shape	Figure	E_{ad}	E_{cl}^{rel}	E_{cl}^{rel}/N	E_{sur}^{rel}	E_{int}
1*		1	−1.00	0.08	0.08	0.76	−1.85
2*			−1.22	0.07	0.04	0.64	−1.92
3*			−1.58	0.09	0.03	0.81	−2.48
4	linear	3(b)	−1.81	0.10	0.03	0.90	−2.81
4*	cubic	3(c)	−1.00	0.07	0.02	0.48	−1.56
5*	linear		−1.96	0.15	0.03	0.99	−3.11
8	linear	4(a)				1.55	−4.89
8	planar					1.40	−4.21
8*	cubic		−1.48	0.12	0.02	0.66	−2.26
11*	planar	4(b)				1.87	−5.67
12	planar					1.83	−5.76
12*	3D linear		−1.55	0.22	0.02	0.76	−2.53
16	3D linear	4(c)	−2.39	0.24	0.02	1.01	−3.63
16*	3D square		−2.05	0.19	0.01	0.91	−3.14
24*	parallelepiped	6(a)	−2.14	0.22	0.01	0.90	−3.27
24	rotation 1	6(b)	−1.70	0.31	0.01	0.87	−2.88
24	rotation 2	6(c)	−1.60	0.21	0.01	0.75	−2.56
32*	parallelepiped		−2.19	0.22	0.01	0.86	−3.27
36*	parallelepiped	5	−2.81	0.38	0.01	1.12	−4.31
48*	parallelepiped		−3.63	0.58	0.01	1.51	−5.72

the main factors which determine the mechanism of their aggregation. Three mechanisms for diffusion of the LiCl and MgO molecules along the (100) MgO surface were considered in Ref. 38. It was demonstrated that two of them, successive "90° reorientations" in the surface plane and "180° out-of-plane rotations" (see Fig. 2), have the lowest and comparable energy barriers. Our present calculations for the NaCl molecule diffusion gave qualitatively similar results. In particular, in-plane 90° reorientations of the NaCl molecule have the smallest adiabatic barriers: reorientation "around" the Cl ion requires us to overcome the barrier of about 0.29 eV, whereas "around" the Na ion requires 0.12 eV. As was discussed in Ref. 38 for the LiCl and MgO molecules, there is a considerable molecular displacement from an ideal rotation configuration and further surface distortion at the transition state (see Fig. 2). The energy barriers for the 180° out-of-plane rotations are equal to about 0.5 and 0.57 eV around the Na and Cl ions, respectively. These energies are much smaller than the molecule adsorption energy at the surface. Therefore one can expect that, in the process of relaxation into the stable adsorption state and energy dissipation, the molecule can make several jumps along the surface.

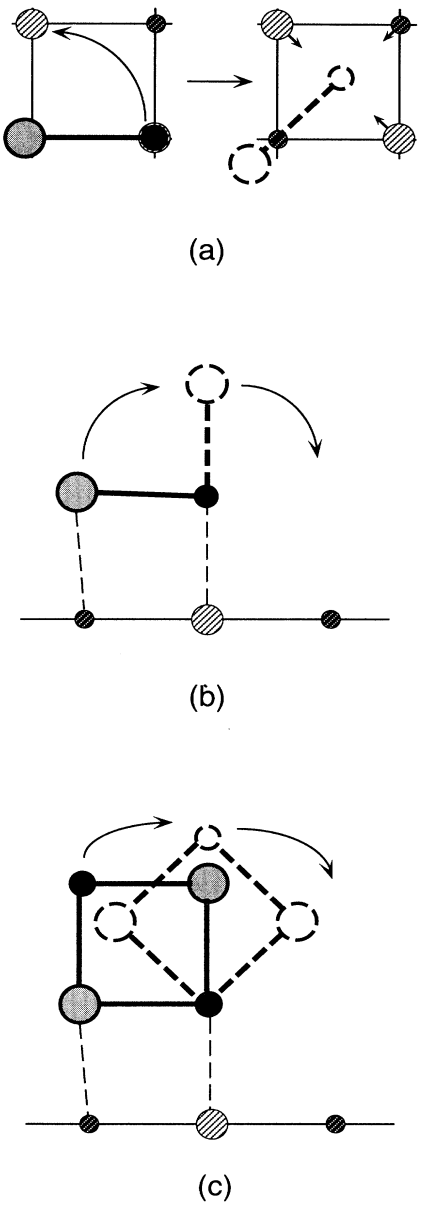

FIG. 2. Schematic diagrams showing diffusion mechanisms (a) 90° in-plane reorientation for one NaCl molecule, (b) 180° out-of-plane rotation for a single NaCl molecule, and (c) rotation of cube around an edge for four NaCl molecules. Barrier-point configurations are shown by bold broken lines. The curved arrows indicate the reorientation pathways. The small arrows in (a) shown the lattice relaxation at the barrier point.

The second molecule can be attached to the first one, already adsorbed at the surface, in three different ways: antiparallel, perpendicular, and linear (along the same surface axis). The most stable configuration is the antiparallel rhombic configuration in which the ions make the largest number of bonds. The attachment energy E_{att} can be defined as the difference $E_{\text{att}} = E_n - E_{n-1} - E_{\text{mol}}$, where E_m is the total energy of the cluster of m ($m = n$ or $n-1$) molecules and the surface, and E_{mol} is the energy of the free NaCl molecule. It characterizes the energy gain due to attachment of the next molecule from the free state to the cluster already adsorbed at the surface. In the rhombic configuration it is about 2.53 eV. For comparison, this is 0.75 eV larger than for the linear configuration in which the molecules are adsorbed in neighboring positions along the ⟨100⟩ surface axis. The binding energy per molecule between the molecules in the adsorbed rhombic dimer is 1.13 eV which is only 0.03 eV smaller than in the free dimer. The rhombic configuration is very close to that of the free dimer and is slightly distorted perpendicular to the surface. In particular, the Na-Cl-Na angle increases from 77.9° to 78.7°, whereas the Na-Cl distance increases from 2.59 to 2.62 Å. For comparison, the experimentally determined geometric parameters of the free dimer are 78.6° and 2.58 Å, respectively.[8] The surface distortion energy is significantly smaller than that for the single molecule because of the much smaller electrostatic interaction. The latter increases considerably after attachment of a third molecule as the cluster reacquires a dipole moment.

The attachment energy for the third molecule in the most stable configuration antiparallel to the adjacent molecule [this geometry is similar to that shown in Fig. 3(a) if one ignores the fourth molecule attached on the left side] is 2.18 eV. However, the energy of this configuration is lower than the energy of the dimer and the individual molecule separately adsorbed at the surface by about 1.18 eV. We note that reaction energy $\text{NaCl} + (\text{NaCl})_2 \rightarrow (\text{NaCl})_3$ calculated for the free molecules is 1.82 eV (1.6 eV according to Ref. 22). The difference is caused predominantly by the large surface distortion. The linear-chain configuration of the three almost antiparallel molecules is one of the two stable configurations which are established for the free NaCl tri-

mer.[22] The other configuration for a free cluster is a ring, which has a very close or even lower energy.[22] For three molecules it has a structure close to the linear chain. The strong interaction with the squared lattice template diminishes the difference between the two configurations and in fact they converge into one.

For the four different configurations of four molecules shown in Fig. 3, the attachment energy is only useful for the first two planar configurations. The first of them has $E_{att}=1.84$ eV, whereas the second configuration has $E_{att}=2.13$ eV. The rearrangement of the cluster from the first into the second configuration requires several successive reorientations of a molecule. However, due to the high attachment energy, the barrier for rotation of the molecule, which limits the rearrangement process, is about 1.0 eV. This makes the rearrangement highly unlikely once the adsorbed molecule(s) are in thermal equilibrium with the substrate. Part of the attachment energy, though, could be used for this rearrangement during the equilibration process. The cluster in the second

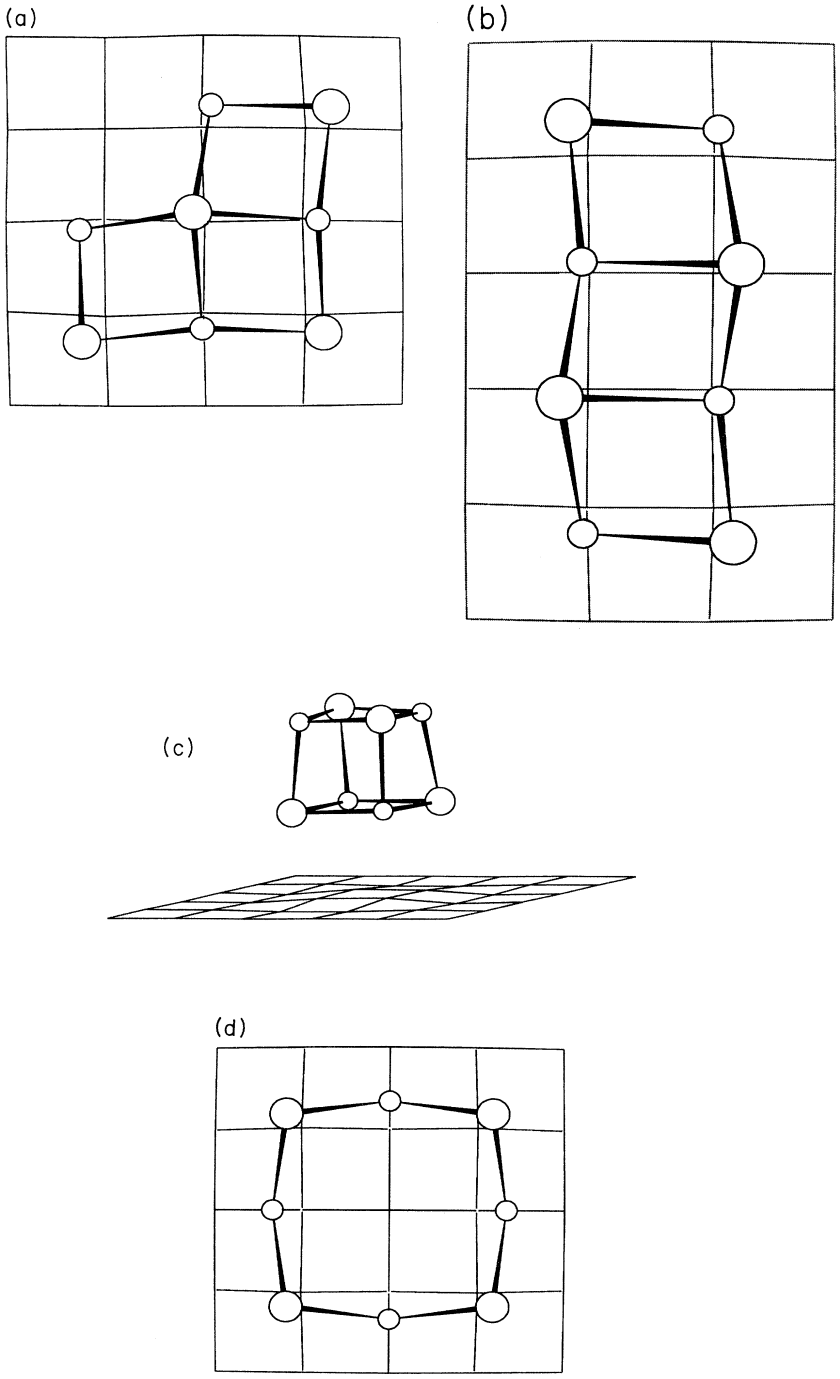

FIG. 3. Optimized geometries for four different configurations of four NaCl molecules on the (100) surface of MgO; (a) planar cluster, (b) linear chain of antiparallel molecules, (c) cube, and (d) ring. Large circles correspond to the Cl^- ions and small circles to the Na^+ ions. The approximate geometry for the $(NaCl)_3$ cluster can be visualized from (a) and (b) by the removal of one molecule.

configuration makes a bridgelike strained structure [see Fig. 3(b)]. The energy of this structure is only 0.11 eV higher than the energy of the most stable cubic structure shown in Fig. 3(c). The latter is strongly distorted with interionic distances in the upper rhomb of 2.66 Å and in the lower rhomb of 2.72 Å. The energy of the ring structure in Fig. 3(d) is 0.59 eV higher than that of the cube. The relative stability of the free clusters[22] and the adsorbed clusters in the same order [Fig. 3(c), 3(b), 3(d)], but the energy differences are much larger for the free clusters. In particular, the energy of the cubic structure is lower than that for the linear chain of antiparallel molecules by 0.83 eV (0.9 eV in Ref. 22). This clearly results from the interaction with the surface. Note that $E_{\text{sur}}^{\text{rel}}$ and E_{int} for the cubic structure are much smaller than for the linear $(NaCl)_4$ structure [Fig. 3(b)] and close to the values for the $(NaCl)_2$ cluster (see Table II). The latter suggests that the molecular pair closest to the surface makes the main contribution to both energies.

These results already reflect several common features which persist for all the clusters studied in this paper. First, the barriers for diffusion of individual molecules along the surface are much smaller than the attachment energies to existing clusters and intracluster interaction energies. Further rearrangement of the cluster structure after a molecule sticks to a particular cluster position in many cases seems to be unlikely. This implies that diffusion-limited aggregation can be the main mechanism of cluster growth and that clusters may have branched fractal features.[62] Therefore, in principle, for a large number of molecules, the number of possible initially formed (meta)stable configurations can be very large. The relative abundance of these structures at real growth conditions depends on the speed of molecular deposition, substrate temperature, and structure. Secondly, the configurations shown in Fig. 3 reveal three characteristic qualitative shapes of the most stable structural fragments obtained in this study: a linear chain of antiparallel-aligned molecules which we will call further a "linear chain" [see Figs. 3(b) and 4(a)], a planar monolayer structure [see Figs. 3(a) and 4(b)], and a three-dimensional two-layered parallelepipedlike structure [see Figs. 3(c), 4(c), 5, and 6]. We will call the latter type "parallelepiped." Finally, the surface deformation produced by clusters extends wider than the projection of the cluster onto the surface. For example, for the linear $(NaCl)_4$

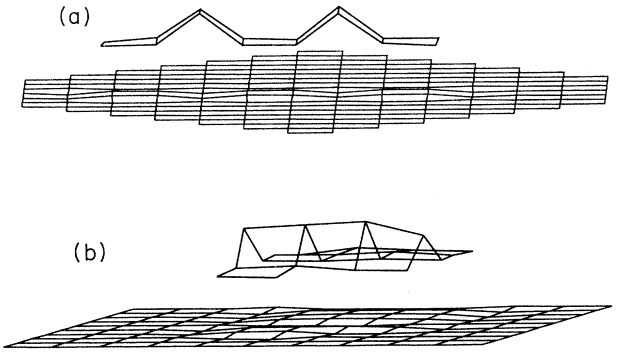

FIG. 4. Equilibrium cluster and surface geometries for (a) linear antiparallel chain of eight molecules, (b) planar array of 11 molecules with kink, and (c) linear three-dimensional two-layered parallelepipedlike structure of 16 molecules.

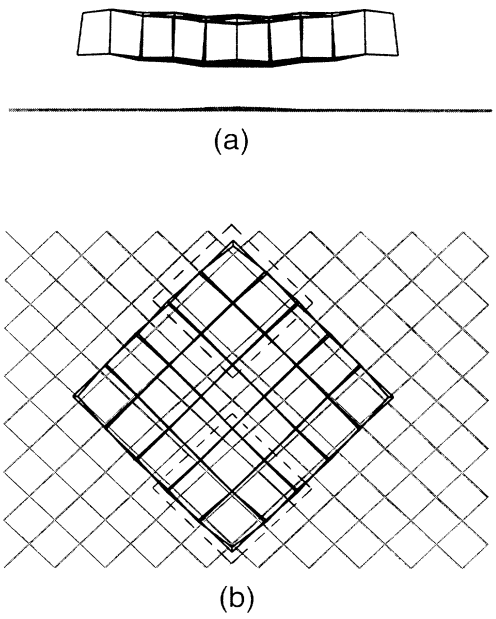

FIG. 5. Two views of the equilibrium geometry of the $(NaCl)_{36}$ cluster on the MgO surface. (a) shows the large cluster distortion perpendicular to the surface. In (b) the areas where there is a correspondence between surface and cluster sites are marked by broken lines.

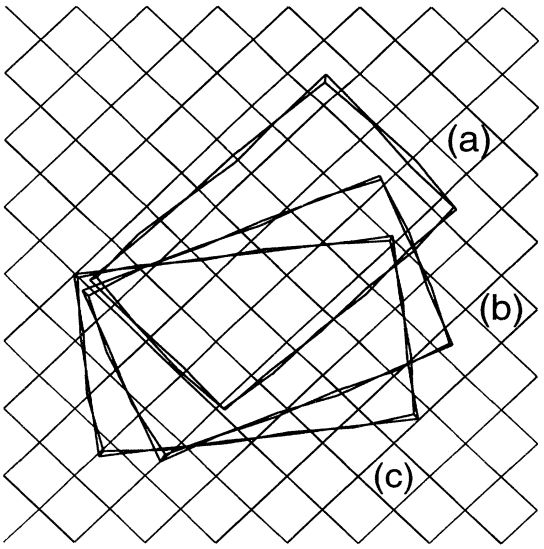

FIG. 6. An overlay of the borders of different orientations of the $(NaCl)_{24}$ cluster on the (100) surface of MgO obtained by rotation about a vertex of cluster (a).

cluster, the surface ions at the edges of Fig. 3(b) are displaced away from the cluster by about 0.04–0.09 Å. Further from the cluster, the displacements are close to zero. For other clusters, the surface deformation typically extends about 1–2 lattice constants wider than the projection of the cluster onto the surface [see, for example, Figs. 4(a) and 4(b)].

B. Comparison with free clusters

The cluster-surface interaction is reflected in the shape of the most stable adsorbed clusters compared to the free clusters of the same number of molecules. The structures of the free $(NaCl)_n$ clusters obtained in Refs. 19 and 22 can be approximately described as parallelepipeds or polygons constructed from NaCl, $(NaCl)_2$, and $(NaCl)_3$ fragments. The most stable configuration of $(NaCl)_2$ is a rhomb. That of $(NaCl)_3$ is a hexagonal ring. The energy of the latter is extremely close to that of the linear-chain configuration with C_{2v} symmetry in which the three molecules are arranged almost antiparallel.[22] For an even number of molecules, the parallelepipedlike structures are the most energetically stable starting at $n=4$. The hexagon-based cylindrical structures in some cases have very close energies to the parallelepipeds, especially when n is divisible by 3. Many of the most stable structures for an odd number of molecules resemble the parallelepipeds with $n-1$ molecules with an attached molecule. Alternatively they may be smaller parallelepipeds which incorporate rhombs and hexagonal rings.[19,22]

As was pointed out previously, the MgO surface makes a template which favors quadrangular structures over hexagonal. Apart from $n=3,5$, the most stable structures of all other clusters adsorbed at the surface obtained in our calculations correspond to the most stable free-cluster structures. The strong interaction with the surface makes the energy of the linear $(NaCl)_5$ structure about 0.1 eV lower than that of the $(NaCl)_4$ cube with an attached NaCl molecule. For the free clusters, the latter was calculated to have the energy 0.66 eV lower than that of the linear chain (0.76 eV in Ref. 22). The linear-chain configuration remains the most stable only for three and five molecules. However, even for eight molecules the total-energy difference between the three types of structures is only about 0.3 eV with the parallelepipedtype structure being the most stable. The planar structures considered in this study included up to 12 molecules. Starting from six molecules this structure is already less energetically profitable than the two-layered parallelepiped structure. These structures may have kink(s) [see, for example, Figs. 7(a) and 4(b)]. The attachment energy of the next molecule to the kink is much larger than that to the linear edge of the cluster. Therefore planar clusters of an even number of molecules and regular shape are more stable than those of odd number. However, starting from six molecules, the parallelepiped struc-

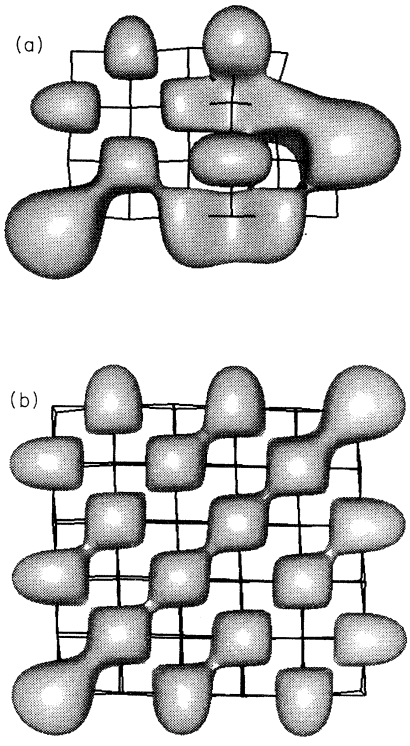

FIG. 7. Three-dimensional electrostatic equipotential surfaces produced by the clusters. (a) Planar cluster of 11 molecules with kink and (b) parallelepiped cluster of 36 molecules. The displayed surfaces correspond to 1.5 eV. In (b), for clarity, only the potential around the top layer of the cluster is drawn.

tures dominating the free-cluster structure also begin to dominate the most stable structures of the adsorbed clusters. This results both from the accumulating misfit and the intracluster interaction. In particular, the binding energy per molecule in the free and adsorbed clusters increases with the cluster size whereas the cluster-surface interaction per interface molecule decreases (see Table II). We discuss these issues in more detail in the next section.

Based on this tendency we considered further only the most compact three-dimensional two-layered parallelepiped clusters of 16, 24, 32, 36, and 48 NaCl molecules. We should stress, however, that many of the linear and planar structures of adsorbed clusters, which do not exist in the free state and are stabilized due to the interaction with the surface, have energies which are only slightly different from those of the adsorbed parallelepiped structures.

C. How does the interaction of the clusters with the surface change with the cluster size?

More detailed information regarding the cluster-surface interaction can be gained from Table II. It can be seen that the total cluster-surface interaction energy generally increases with the cluster size. To compare the E_{int} for the linear, planar, and parallelepiped structures we divided this energy by the number of cluster molecules in direct contact with the surface. Although we should note that due to the cluster bending [see Figs. 4(a) and 4(b) and the next section for discussion] this characteristic is approximate, we believe that it reflects the general tendency. As is clear from Table II, the $E_{\text{int}}^{\text{mol}}$ decreases as the interface area increases. The total surface distortion energy on average changes much less than the cluster-surface interaction energy despite the striking difference in cluster shape and size. Since the surface deformation distributes over a larger area than the projection of the cluster, it is difficult to define the interface area. However, it is clear that the surface distortion energy per interface area also decreases rapidly as the cluster size increases. These features reflect the transition from the strong interaction for a single molecule to an interfacial interaction between two crystal surfaces with large misfit.

The electrostatic interaction between a cluster and the surface makes one of the major contributions to the interaction energy. The interference of the Coulomb contributions from the individual ions decreases the electrostatic potential at a particular distance from a cluster as its size increases. However, the potential near low-coordinated ions at edges and corners decays more slowly than that below the middle of the cluster where the ions are coordinated more strongly. This point is illustrated in Fig. 7 where the surfaces of equivalent Coulomb potential around the clusters of 11 and 36 molecules are presented. It can be seen that the potential in the internal part of the regular 36-molecule cluster clearly resembles the periodic exponentially decaying potential characteristic for the perfect infinite surface. Its numerical value at a distance of 2.8 Å from the cluster is only about 10% higher than that for the perfect lattice of the same charges. The strong interactions of the corner and edge ions with the surface can bend the cluster shape, and the strong electrostatic potential produced by the kink must impose anisotropy for molecules migrating towards the cluster. Finally, we should note that the van der Waals contribution to the adsorption energy is significant even for small clusters. For clusters larger than those considered in this paper it can become bigger than the electrostatic contribution. However, the van der Waals interaction begins to depend on the ion position with respect to the surface only when the ion-surface distance is less than approximately the surface lattice constant. Therefore it does not affect strongly the cluster geometry at the surface. In particular, for the three different orientations of the $(NaCl)_{24}$ cluster shown in Fig. 6 the van der Waals contribution to the cluster-surface interaction energy changes by only 0.3 eV, whereas the electrostatic contribution changes by 1.45 eV (see the next section).

The energetic characteristics provide, however, only averaged information concerning the cluster-surface interaction. To get a deeper insight into the individual features of particular clusters we will now turn to their geometric structure.

D. How do strained clusters accommodate the strain?

This question is closely related to another question: at which cluster size do the adsorbed molecules lose their identity? If we look at the perfect surface as a probe of cluster structure we can restate this question as follows: at which cluster size does the molecule-surface interaction characteristic for adsorption transfer into the solid-solid interaction characteristic for an interface? We address these questions by analyzing the character of the cluster deformation.

There is a striking difference between the structures of the linear, planar, and three-dimensional clusters of the same number of molecules in direct contact with the surface. In the first two types of cluster, the corner ions tend to maintain their correspondence with the surface ions of opposite charge. Because of the strong misfit with the surface along the length of linear clusters, they release the strain by forming rooflike structures in which some molecules are repelled up out from the plane as shown for the eight-molecule cluster in Fig. 4(a). For a large number of molecules, the planar structures stabilized by bending perpendicular to the surface similarly to the linear structures, as shown in Fig. 4(b) for 11 molecules. Although we only considered linear and planar clusters up to 12 molecules, we believe that much larger clusters can be stabilized in this way as well.

The internal structure of the three-dimensional clusters is more rigid. The upper layer in these clusters weakly

interacts with the surface and bends in order to accommodate the strain [see, for example, Fig. 5(a)]. This is enough to minimize the strain for the clusters of six and eight molecules. However, the larger linear clusters bend along the surface as shown in Fig. 4(c) for 16 molecules. Although they already interact with the surface like crystal blocks they still bear strong molecular-cluster features. To clarify this and other points we will consider the cluster $(NaCl)_{36}$ in more detail.

The ratio between the bulk lattice constant of NaCl and MgO is equal to 1.337 which approximately corresponds to 6 lattice units of NaCl per 8 lattice units of MgO along the ⟨100⟩ surface axis. Therefore formally one could expect a good geometric correspondence between the corners of the squared $(NaCl)_{36}$ cluster and the surface lattice sites as the side of the cluster is 6 interionic distances long. However, as one can see in Fig. 5(b), the correspondence between the cluster corners and the surface sites is in fact approximately 6:7. This illustrates the point as to how fast the geometric parameters of the cluster approach the bulk crystal values as the cluster size increases. The distances between the nearest ions in the cluster interior are approximately equivalent and equal about 2.71 Å. Those between the inner ions and those at the cluster edges are equal to 2.69 Å. The distances between the nearest ions at the corners on the upper plane are 2.67 Å and these on the lower plane are 2.62 Å. These parameters are still much smaller than the calculated bulk lattice constant, which is equal to 2.815 Å. They also reflect the considerable cluster distortion at the corners which is notable in Fig. 5. Due to the strong misfit there is relatively good correspondence between the opposite-sign cluster and surface ions only at the two cluster corners shown by the broken lines. The two other corners are located approximately above the sites with the same ion charge. Because of the electrostatic repulsion at these corners the cluster is considerably twisted [see Fig. 5(a)]. In particular, the difference in height from the surface for the two types of corners is equal to 0.65 Å.

The strong distortion of the $(NaCl)_{36}$ cluster due to the electrostatic repulsion at the corners, the peculiar distortion of the planar clusters [see Figs. 4(a) and 4(b)], and the difference in the electrostatic potential between the cluster edges, corners, and interior (see Fig. 7) seem to suggest that the interaction of the low-coordinated cluster sites with the surface can strongly influence the cluster geometry and orientation at the surface. In order to understand this point better and to study other possible cluster configurations at the surface we considered different orientations of the less symmetric $(NaCl)_{24}$ cluster shown in Fig. 6. The first configuration of this cluster has its edges roughly parallel to the ⟨100⟩ surface axis and a quite poor correspondence between the cluster and the surface ions of the opposite sign. The cluster bends strongly both parallel and perpendicular to the surface plane in order to improve the correspondence and to reduce the electrostatic repulsion. In particular, the distance from the surface for the ions with a "good" correspondence with the surface ions is about 2.89 Å, whereas the ions in the opposite cluster corner are 3.69 Å from the surface. To find a better correspondence between the corner ions of the cluster with the surface ions we rotated the cluster with respect to the surface and minimized the total energy. Two stable configurations which satisfy both criteria are shown in Figs. 6(b) and 6(c). The first of these configurations has the total energy 0.44 eV higher, and the second configuration 0.55 eV higher than the energy of the initial configuration. As one can see from Table II, both of the rotated configurations have lower surface distortion energies. However, the cluster-surface interaction energies are in both cases much smaller. This results from the fact that after rotation there is no area of a good cluster-surface ion correspondence except for the few scattered ions and the cluster corners (see Fig. 6). As a result the electrostatic contribution to the interaction energy decreases from -3.44 eV for the initial configuration to -1.99 eV for the configuration shown in Fig. 6(c).

Turning back to Table II and Figs. 3–7 it becomes more apparent that qualitatively speaking the bigger the area of a good correspondence between the cluster and surface ions of the opposite sign the larger the cluster-surface interaction energy. Similar electrostatic requirements for anion-cation near-neighbor pairs at the interface were discussed recently in Ref. 63. We should note that because of the misfit only an approximate correspondence is possible for large areas. For instance, the best such correspondence exists for the $(NaCl)_{16}$ cluster which can be viewed as four cubes arranged in a square configuration. However, as one can see in Table II, the cluster-surface interaction energy for this cluster is less than two times larger than that for the cube. The same is true for the dimer and the linear configuration of the tetramer.

These results demonstrate also that the bulk-crystal geometric parameters can be achieved only at much larger cluster sizes. It seems tempting to interpolate our data in order to find approximately this cluster size. However, closer analysis shows that the cluster sizes considered in this work are still too small for reliable conclusions. First, the interionic distance changes only from 2.66 to 2.71 Å as the cluster size increases from 4 to 48 molecules. Secondly, the number of interior ions in the clusters smaller than 36 molecules is small and their shape is strongly affected by the size and their interaction with the surface.

E. Cluster diffusion

Another way to probe the cluster interaction with the surface is to calculate the adiabatic potential-energy surface for cluster displacements along the surface. In particular, one can expect that the adiabatic potential for their displacement in certain directions can be very flat since the electrostatic potential of the large clusters is incoherent with that of the surface. For comparison we calculated the adiabatic potentials for the displacements of the cubic $(NaCl)_4$ cluster shown in Fig. 3(c) and those for the parallelepiped $(NaCl)_{36}$ cluster (see Fig. 5) along the ⟨100⟩ and ⟨110⟩ surface axes. In these calculations one of the cluster ions was fixed at a certain trajectory point whereas all other cluster and surface ions were al-

lowed to find new positions in which the forces at these ions were zero. The barrier point was found at zero forces exerted at all cluster and surface ions including the fixed ion.

The bottom ions of the $(NaCl)_4$ cubic cluster in its most stable configuration at the surface strongly interact with the corresponding surface ions with the opposite sign. This configuration has a symmetry axis perpendicular to the surface and passing through the middle of the Mg_2O_2 surface unit and the cluster. Therefore all Mg_2O_2 surface units in the $\langle 100 \rangle$ direction are equivalent with respect to the $(NaCl)_4$ cluster translations. The barrier point occurs when the center of the cluster lies above the cation or anion site at $0.71a$ from the initial cluster position, where a is the interionic surface distance. The value of the calculated barrier energy for the displacement of the $(NaCl)_4$ cluster between the equivalent surface positions is 0.39 eV.

The length of the vector corresponding to the translation of the cluster between equivalent positions in the $\langle 100 \rangle$ direction is equal to $2a$. However, in fact the direct translation does not take place but the cluster tends to rotate over a corner or edge. The latter process is schematically depicted in Fig. 2(c). It provides the shortest path for the cluster displacement along the $\langle 100 \rangle$ axis and has a barrier energy equal to 0.36 eV. The rotation over the corner in fact leads to the cluster displacement along the $\langle 110 \rangle$ axis. The calculated barrier for this rotation is about 0.73 eV. It is interesting to note that the barrier energies for the translations of the $(NaCl)_4$ cluster along the surface are not much higher than those for the individual molecule.

Due to the symmetry of the adsorption state of the $(NaCl)_{36}$ cluster at the surface [see Fig. 5(b)] all cluster translations on the intersite distance along the $\langle 110 \rangle$ axis are equivalent. The translational displacement of the $(NaCl)_{36}$ cluster along the $\langle 110 \rangle$ direction requires overcoming a barrier of 0.37 eV. The cluster displacement on the surface lattice constant along the $\langle 100 \rangle$ axis also brings it into the equivalent position. However, the correspondence of the cluster ions with those at the surface changes between the different cluster corners. Therefore the displacement of the cluster is accompanied by its twisting. The calculated barrier for the cluster translation along the $\langle 100 \rangle$ direction is only 0.14 eV.

IV. DISCUSSION

In this section we will consider possible implications of the results of this study with respect to the different properties of insulator-insulator adsorption and interfaces. First, we will compare the structural and energetic properties of the clusters studied in this paper with the results of other cluster studies and MBE of AH's. Then we will briefly consider their electronic structure and optical characteristics, and the possibility of their observation using AFM.

A. Cluster structural properties and film growth

Epitaxial growth of wide-gap insulating materials such as alkali halides and simple ionic oxides provides a very interesting example of the MBE of nonmonatomic species. In particular, it has been demonstrated experimentally that thin films and excellent single crystals of several alkali halides and MgO can be grown by MBE even at temperatures as low as about 100 K.[26,27] It has been suggested that this unusually low-temperature growth may be due to very high mobility of surface species.[26] An activation energy of the order of 0.1 eV has been estimated for the mobility of KCl molecules on a surface terrace of KCl.[26] The calculated adiabatic barriers for diffusion of LiCl and MgO single molecules[38] and NaCl molecules on the surface of MgO, which are about 0.3 eV, confirm the generally high mobility of molecular species on surface terraces of cubic ionic materials. Large adsorption energies of these molecules and big surface deformation energies obtained in this study (see Table II) suggest that the high mobility of the primary adsorbed species may be partly due to their "hot" jumps during energy dissipation. This point requires more careful study using molecular-dynamics techniques which are currently in progress in this group.

Heteroepitaxy of alkali halides on the surface of alkali halides has been studied recently using high-resolution He-atom scattering.[28–30] In particular, oscillations in the intensity of the specular beam due to layer-by-layer growth were observed for the first several layers of KBr growth on the (100) NaCl surface.[28] However, the diffraction pattern after the deposition of two layers shows peaks with both the NaCl and superstructure corrugation and very small specular intensity. By six layers the specular is much larger, indicating a considerably better surface. The surface lattice spacings for NaCl and KBr have a large mismatch of about 17%. Therefore to explain the data for the first two layers it was suggested that they should contain many defects or very small islands. In particular, it has been proposed that the KBr molecules initially deposit oriented normal to the surface, forming small bilayer patches that buckle and give rise to the superstructure, but in subsequent layers they align parallel to the surface. The results of the present study qualitatively support this model. They suggest that at large mismatch and strong intermolecule interaction initial formation of the bilayer structures is more plausible than that of the monolayer. The cluster bending both along and perpendicular to the surface shown in this paper can give rise to formation of defects and dislocations.

We should note that the clusters considered in this study are most probably much smaller than the "small islands" proposed in Ref. 28. However, another interesting question is how are these islands and the next layers of adsorbed material oriented with respect to the substrate lattice axis, and how does the structure of initial fragments determine the structure of the thick film? This question is related to a near-coincident-site-lattice model developed for noncommensurate heteroepitaxial interfaces.[64] According to this model various two-dimensional coincidence-site lattices can be produced by rotating one lattice with respect to the other about the axis normal to the interface until three nonlinear lattice sites of the two materials are in coincidence. This procedure gives a set of initial formal geometries of the interface which should

be further optimized taking into account the interionic interactions and using energy-minimization techniques. This procedure seems to be appropriate for the calculation of the interaction between two macroscopic surfaces and grain boundaries and was recently applied to the study of the BaO/MgO interface.[64] It concludes that for the best site coincidence at large misfits two lattices can be rotated with respect to each other.

Unfortunately, both the experimental data on the KBr/NaCl interface[28] and the theoretical results of the present work do not give a conclusive answer to the question posed in the previous paragraph. From the He-atom-scattering (HAS) data one can construct the surface phonon dispersion curves.[28] The experimental data and the results of analysis of phonon spectra performed in Refs. 28 and 29 seem to suggest that for several layers of KBr the main surface axes of both lattices are parallel. However, the experimental details given in Refs. 28 and 29 are not enough to reach a final conclusion. The results of the present calculations demonstrate that at molecular deposition very small clusters are already very stable at the surface and can act as nucleation sites. The latter will grow further by the attachment of new molecules. At initial stages of this growth (at least until 16 molecules in this study) the clusters tend to align with there edges parallel to the surface axis. However, there is a clear tendency for the larger clusters to bend along the surface. Therefore the shapes of the real clusters and islands can be complicated. This point requires statistical simulation of the cluster growth which is out of the scope of this paper.

However, we should point out that these results demonstrate clearly that the formal "misfit" between the lattice constants of the substrate and the deposited material strongly depends on the cluster size. According to our results, rotation of the large clusters to satisfy new coincidence-site lattice conditions appropriate for their size seems unlikely. It is also interesting to note in this respect that the cluster distortion energies obtained in our calculations are much smaller than the corresponding surface distortion energies (see Table II). This is despite the fact that some of the clusters are strongly deformed compared to their geometry in the free state. Apart from the reasons discussed in the previous section, this is caused by the fact that because of its continuity the *lattice* deformation spreads over a bigger area than that of the cluster. Therefore gaps between clusters can decrease the overall strain energy and their existence is energetically profitable. Thus island formation, their buckling, and formation of dislocations seems to be a realistic model for the first MBE layers, as discussed in Ref. 28. However, HAS cannot give any definite answers regarding the structure of small islands. Some additional information in this respect could be gained from spectroscopic and AFM measurements.

B. Cluster electronic structure

In this work we are particularly interested in the possibility of the identification of the clusters at surfaces using optical absorption and other spectroscopic techniques. This is only possible if there is a considerable dependence of the cluster optical properties on their size. This dependence has been demonstrated experimentally for wide-gap semiconductors, such as CdS.[3] The transition from the electronic structure of single adsorbed NaCl molecules to the well-known bulk structure has been studied recently for thin adlayers deposited on W(110) using electron energy-loss spectroscopy (EELS), MIES, and other spectroscopic techniques.[34] However, similar studies on dielectric substrates such as MgO are much more difficult because of surface charging. The question which arises is where the holes created in the Auger process will be localized.

To address these questions we calculated the electronic structure and optical-absorption energies for the clusters of $n=1,2,4,32,48$ NaCl molecules, the infinite bulk lattice of NaCl, and the (100) surface of MgO. The cluster one-electron states form a discrete energy spectrum. We calculated the one-electron transitions been these states using a configuration-interaction technique similar to that discussed in Ref. 58. They form a spectrum which includes transitions with different transition matrix elements. For our present purpose we are primarily interested in the "strong" transitions, i.e., in those with the largest transition matrix elements, which fall in the optical band gap of the MgO (100) surface. The latter was calculated to be 7.9 eV. The energies of the lowest "strong" transitions for the free NaCl clusters of n molecules with $n=1$, 2, 4, 32, and 48 are 5.5, 6.8, 7.6, 7.2, and 7.7 eV. The calculated optical band gap for bulk NaCl is 8.7 eV (8.6 eV is the experimental value[65]). For the 32- and 48-molecule clusters the lowest transitions correspond to the electronic states delocalized by the low-coordinated corner ions. The transitions corresponding to the "internal" cluster ions have energies about 8.1 and 8.2 eV, respectively, i.e., much closer to the bulk value. These data demonstrate that the optical "band gap" increases as the cluster size increases and is distinctly different from the bulk NaCl value for the small clusters.

For these clusters adsorbed at the surface, there is a "tail" of cross transitions corresponding to the electron transfer from the surface oxygen states perturbed by the cluster to the cluster sodium states perturbed by the surface. They have energies in the range of 6.1–6.9 eV, and smaller transition matrix elements than the intracluster transitions. The cluster perturbation is reflected in the redshift of the strongest transition. In particular, in the four-molecule cube the energy of this transition decreases from 7.6 to 7.1 eV. The low-energy cross transitions persist for all clusters considered. We should note, however, that they appear because the bottom of the conduction band in the bulk of NaCl in our calculations lies lower than that of the bulk and surface of MgO. There are presently not enough theoretical or experimental data to conclude whether this is correct. Based on these data and the results of previous calculations[66,67] we can conclude that, although the optical-absorption energies of the small clusters are smaller than the band gap of bulk MgO, they are likely to mix with the surface states of the real MgO surface containing steps and kinks and with the excitonic bands which have much lower energies. On the other hand, they could be observed in the case of the oth-

er substrates with higher surface excitation energies [9.2 eV for NaF and 10.2 eV for LiF (Ref. 68)]. The fact that chlorine valence states lie much lower than the top of the oxygen valence band implies that the holes produced in MIES and similar experimental techniques based on Auger processes will localize in the substrate. However, this point requires more careful calculation of the self-trapping energy.[69]

C. Possibility of the AFM observation

It is tempting to suggest application of the AFM technique to the study of small clusters at insulating surfaces. This could be the only direct way to study the geometry of individual clusters and the very initial stages of film growth. The crucial issue which determines the very possibility of the observation of clusters at surfaces is the tip-cluster interaction. A small cluster can be adsorbed on the tip or displaced by it along the surface. One can, at least in principle, try to avoid the first problem by choosing the tip material. However, the second problem seems to be more fundamental. This can be understood from the experimental fact that the friction forces exerted on the tip when it climbs the surface step are considerably larger than these when it scans down the step.[70]

We have calculated the maximum forces necessary to displace the 4- and 36-molecule clusters between their stable configurations along the ⟨100⟩ and ⟨110⟩ surface axes. They are equal to 0.9 and 0.3 nN along the ⟨100⟩ axis, and 0.6 and 0.7 nN along the ⟨110⟩ axes, respectively, for the $(NaCl)_4$ cluster and the $(NaCl)_{36}$ cluster. The experimentally measured friction force exerted on the AFM cantilever scanning up a two-layer step on the (100) NaCl surface is about 9 nN,[70] i.e., more than an order of magnitude bigger. Although this is not exactly the same system we believe that this comparison is meaningful. One can see that the tip can easily move even relatively large clusters along the surface during scanning. This implies that one can expect to observe clusters mainly at surface steps and kinks.

Finally, we should note that many of the qualitative results obtained in this study with respect to the structure, properties, and possibilities of experimental observation of clusters at ionic surfaces should be valid for a wide range of alkali halides and cubic ionic oxides where the intramolecular separation exceeds the substrate lattice parameter. We believe that further development of experimental techniques will allow the study of trapping of electrons and holes in these and similar adsorbed clusters, chemical reactions of adsorbed clusters with molecules, and photoinduced processes which are already in progress for free clusters and surfaces.[9,12,71]

ACKNOWLEDGMENTS

A.L.S. acknowledges SERC, Latvian Scientific Council (Grant No. 93.270), and Deutsche Forschungsgemeinschaft (Contract No. 436 LET 113) for financial support. A.L.R. was supported by SERC and ICI. D.H.G. would like to thank Biosym Technologies for their financial support. The authors are indebted to R. W. Grimes and J. Binks for deriving the pair potentials used in this study. We are grateful to C. R. A. Catlow, D. C. Sayle, V. Kempter, L. Howald, R. Luethi, and A. Baratoff for useful discussions. We want to thank Biosym Technologies, San Diego and Cherwell Scientific, Oxford for supplying the computer codes used for the graphical representations in this study.

[1]J. C. Phillips, Chem. Rev. **86**, 619 (1986).
[2]M. Bixon and J. Jortner, J. Chem. Phys. **91**, 1631 (1989).
[3]Y. Wang and N. Herron, J. Phys. Chem. **95**, 525 (1991).
[4]S. H. Tolbert and A. P. Alivisatos, Science **265**, 373 (1994).
[5]Y. J. Twu, C.W. S. Conover, Y. A. Yang, and L. A. Bloomfield, Phys. Rev. B **42**, 5306 (1990).
[6]P. J. Ziemann and A. W. Castleman, Jr., Z. Phys. D **20**, 97 (1991).
[7]J. E. Campana, T. M. Burlak, R. J. Colton, J. J. DeCorpo, J. R. Wyatt, and B. I. Dunlap, Phys. Rev. Lett. **47**, 1046 (1981).
[8]R. J. Mawhorter, M. Fink, and J. G. Hartley, J. Chem. Phys. **83**, 4418 (1985).
[9]E. C. Honea, M. L. Homer, P. Labastie, and R. L. Whetten, Phys. Rev. Lett. **63**, 394 (1989).
[10]R. D. Beck, P. S. John, M. L. Homer, and R. L. Whetten, Science **253**, 879 (1991).
[11]M. L. Homer, F. E. Livingston, and R. L. Whetten, J. Am. Chem. Soc. **114**, 6558 (1992).
[12]X. Li, R. D. Beck, and R. L. Whetten, Phys. Rev. Lett. **68**, 3420 (1992).
[13]P. J. Ziemann and A. W. Castleman, Jr., Phys. Rev. B **44**, 6488 (1991).
[14]P. J. Ziemann and A. W. Castleman, Jr., J. Chem. Phys. **94**, 718 (1991).
[15]P. J. Ziemann and A. W. Castleman, Jr., J. Phys. Chem. **96**, 4271 (1992).
[16]H. W. Sarkas, S. T. Arnold, J. H. Hendricks, L. H. Kidder, C. A. Jones, and K. H. Bowen, Z. Phys. D **26**, 46 (1993).
[17]D. O. Welch, O. W. Lazareth, and G. J. Dienes, J. Chem. Phys. **68**, 2159 (1978).
[18]Y. Wang, P. Nordlander, and N. H. Tolk, J. Chem. Phys. **89**, 4163 (1988).
[19]N. G. Phillips, C. W. S. Conover, and L. A. Bloomfield, J. Chem. Phys. **94**, 4980 (1991).
[20]P. Weis, C. Ochsenfeld, R. Ahlrichs, and M. M. Kappes, J. Chem. Phys. **97**, 2553 (1992).
[21]S. Moukouri and C. Noguera, Z. Phys. D. **24**, 71 (1992).
[22]C. Ochsenfeld and R. Ahlrichs, J. Chem. Phys. **97**, 3487 (1992).
[23]J. P. Rose and R. S. Berry, J. Chem. Phys. **96**, 517 (1992).
[24]J. M. Recio, R. Pandey, A. Ayuela, and A. B. Kunz, J. Chem. Phys. **98**, 4783 (1993).
[25]P. S. Bagus, F. Illas, and C. Sousa, J. Chem. Phys. **100**, 2943 (1994).
[26]M. H. Yang and C. P. Flynn, Phys. Rev. Lett. **62**, 2476 (1989).
[27]S. Yadavali, M. H. Yang, and C. P. Flynn, Phys. Rev. B **41**, 7961 (1990).
[28]J. Duan, G. G. Bishop, E. S. Gillman, G. Chern, S. A. Safron,

and J. G. Skofronick, Surf. Sci. **272**, 220 (1992).
[29]S. A. Safron, G. G. Bishop, J. Duan, E. S. Gillman, and J. G. Skofronick, J. Phys. Chem. **97**, 2270 (1993).
[30]S. A. Safron, J. Duan, G. G. Bishop, E. S. Gillman, and J. G. Skofronick, J. Phys. Chem. **97**, 1749 (1993).
[31]G. Binnig, C. F. Quate, and C. Gerber, Phys. Rev. Lett. **56**, 930 (1986).
[32]G. Binnig, Ultramicroscopy **42-44**, 7 (1992).
[33]W. M. Tong, R. S. Williams, A. Yanase, Y. Segawa, and M. S. Anderson, Phys. Rev. Lett. **72**, 3374 (1994).
[34]S. Dieckhoff, H. Muller, W. Maus-Friedrich, H. Brenten, and V. Kempter, Surf. Sci. **279**, 233 (1992).
[35]R. B. Bjorklund, J. E. Lester, and K. G. Spears, J. Chem. Phys. **66**, 3426 (1977).
[36]R. B. Bjorklund and K. G. Spears, J. Chem. Phys. **66**, 3437 (1977).
[37]R. B. Bjorklund and K. G. Spears, J. Chem. Phys. **66**, 3448 (1977).
[38]A. L. Shluger, J. D. Gale, and C. R. A. Catlow, J. Phys. Chem. **96**, 10 389 (1992).
[39]V. Celli and G. Urzua, J. Phys. Condens. Matter **5**, B91 (1993).
[40]D. H. Gay and A. L. Rohl, J. Chem. Soc. Faraday Trans. **91**, 925 (1995).
[41]A. L. Shluger, A. L. Rohl, D. H. Gay, and R. T. Williams, J. Phys. Condens. Matter **6**, 1825 (1994).
[42]A. L. Shluger, Theor. Chim. Acta **66**, 355 (1985).
[43]A. L. Shluger and E. V. Stefanovich, Phys. Rev. B **42**, 9664 (1990).
[44]E. V. Stefanovich, E. K. Shidlovskaya, A. L. Shluger, and M. A. Zakharov, Phys. Status Solidi B **160**, 529 (1990).
[45]P. W. Tasker, Philos. Mag. A **39**, 119 (1979).
[46]B. G. Dick and A. W. Overhauser, Phys. Rev. **112**, 90 (1958).
[47]E. K. Shidlovskaya, E. V. Stefanovich, and A. L. Shluger, Sov. J. Phys. Chem. **62**, 1352 (1988).
[48]D. M. Heyes, M. Barber, and J. H. R. Clarke, J. Chem. Soc. Faraday Trans. 2 **73**, 1485 (1977).
[49]D. J. Binks, Ph.D. thesis, University of Surrey, 1994.
[50]R.W. Grimes, C. R. A. Catlow, and A. M. Stoneham, J. Phys. Condens. Matter **1**, 7367 (1989).
[51]J. H. Harding and A. H. Harker (unpublished).
[52]P. W. Fowler, P. J. Knowles, and N. C. Pyper, Mol. Phys. **56**, 83 (1985).
[53]*Computer Simulation of Solids,* edited by C. R. A. Catlow and W. C. Mackrodt (Springer, Berlin, 1982), Vol. 166.
[54]W. C. Mackrodt, J. Chem. Soc. Faraday Trans. 2 **85**, 541 (1989).
[55]J. D. Gale (unpublished).
[56]R. A. Evarestov, *Quantum-Chemical Methods of Solid State Theory* (Leningrad University Press, Leningrad, 1982).
[57]J. A. Pople and D. L. Beveridge, *Approximate Molecular Orbital Theory* (McGraw-Hill, New York, 1970).
[58]J. B. Foresman, M. Head-Gordon, and J. A. Pople, J. Phys. Chem. **96**, 135 (1992).
[59]A. N. Ermoshkin, E. A. Kotomin, and A. L. Shluger, J. Phys. C **15**, 847 (1982).
[60]M. Causa, R. Dovesi, and F. Ricca, Surf. Sci. **232**, 399 (1990).
[61]C. P. Flynn, Phys. Rev. Lett. **57**, 599 (1986).
[62]R. Jullien, Contemp. Phys. **28**, 477 (1987).
[63]R. A. McKee, F. J. Walker, E. D. Specht, J. G. E. Jellison, L. A. Boatner, and J. H. Harding, Phys. Rev. Lett. **72**, 2741 (1994).
[64]T. X. T. Sayle, C. R. A. Catlow, D. C. Sayle, S. C. Parker, and J. H. Harding, Philos. Mag. A **68**, 565 (1993).
[65]C. B. Lushchik and A. C. Lushchik, *Decay of Electronic Excitations with Defect Formation in Solids* (Nauka, Moscow, 1989).
[66]A. L. Shluger, C. R. A. Catlow, R. W. Grimes, and N. Itoh, J. Phys. Condens. Matter **3**, 8027 (1991).
[67]V. Puchin, A. L. Shluger, Y. Nakai, and N. Itoh, Phys. Rev. B **49**, 11 364 (1994).
[68]K. Saiki, W. R. Xu, and A. Koma, Surf. Sci. **287/288**, 644 (1993).
[69]A. L. Shluger and A. M. Stoneham, J. Phys. Condens. Matter **5**, 3049 (1993).
[70]L. Howald, Ph.D. thesis, University of Basel, 1994.
[71]S. K. Dunn and G. E. Ewing, Chem. Phys. **177**, 571 (1993).

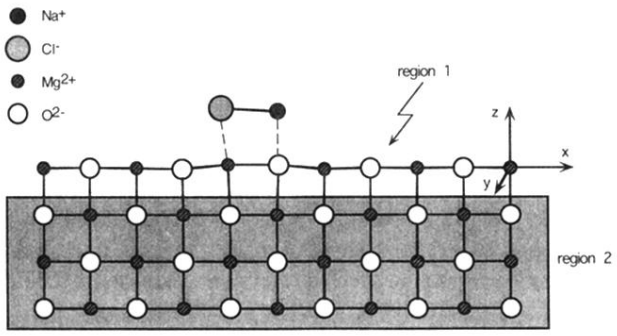

FIG. 1. Part of the simulation cell for the calculation of the adsorption of a molecule of NaCl onto the (100) plane of MgO. The cell is repeated infinitely in the x and y directions.